

Short Communication

Simple Preparation of Co_3O_4 with a Controlled Shape and Excellent Lithium Storage Performance

Yingjie Zhang¹, Huaicong Yan¹, Jiaming Liu², Xue Li^{1,*}, Yiyong Zhang^{1,*}

¹ National and Local Joint Engineering Laboratory for Lithium-ion Batteries and Materials Preparation Technology, Faculty of Metallurgical and Energy Engineering, Kunming University of Science and Technology, Kunming 650093, PR China

² School of Metallurgy and Chemistry Engineering, Jiangxi University of Science and Technology, Ganzhou 341000, PR China

*E-mail: 438616074@qq.com, 810543061@qq.com

Received: 3 January 2020 / Accepted: 9 February 2020 / Published: 10 March 2020

Co_3O_4 and $\text{Co}(\text{OH})_2$ precursors with spherical and a coexisting sheet-spherical morphologies were efficiently prepared using room-temperature deposition combined with calcination. Compared with spherical Co_3O_4 , coexisting sheet-spherical Co_3O_4 has better crystallinity and outstanding lithium storage performance. The first discharge capacity reaches 1089 mAh g^{-1} . The charging capacity is 604 mAh g^{-1} , demonstrating a 50-cycle capacity retention of 70%. The enhanced lithium-ion storage capacity is attributed to the two-dimensional structure of the coexisting sheet and spherical morphology contained in the sheet material; additionally, the surface has a large surface area. Thus, the coexisting sheet-spherical morphology can alleviate the volume expansion caused by lithium-ion insertion, while retaining a high capacity and good cycling performance.

Keywords: Co_3O_4 , Sheet and spherical, Two-dimensional, Lithium ion battery

1. INTRODUCTION

In the early stage of research, transition metal oxides (SnO_2 , Co_3O_4 , TiO_2 , etc.) were found to have reversible charge and discharge capabilities. However, due to their high redox potential and low electrical conductivity, transition metal oxides did not attract attention from the beginning [1-5]. It was not until 1994 when Fuji Corporation first used SnO_2 as a negative electrode material to prepare lithium-ion batteries with discharge capacity reached 600 mAh g^{-1} [6]. To date, research on transition metal oxides has aroused wide interest from scientific researchers due to their high theoretical capacities (SnO_2 : 780 mAh g^{-1} , Co_3O_4 : 890 mAh g^{-1}). Furthermore, their high redox potential can effectively inhibit the formation of lithium dendrites, thus greatly improving the safety performance of the battery.

In recent years, Co_3O_4 has received widespread attention because of its high theoretical capacity. The lithium storage capacity of Co_3O_4 is closely related to its morphology and structure. Researchers have attempted different methods to refine the morphology and structure. For instance, Deng J's group prepared nanosheet-shaped Co_3O_4 by a template method. Its initial capacity was $1735.4 \text{ mAh g}^{-1}$ [7]. Wang B's group prepared a nano straw-like Co_3O_4 material by using a hydrothermal method. The capacity stayed at 842.9 mAh g^{-1} after 300 cycles [8]. Li X's group prepared one-dimensional layered porous Co_3O_4 nanorods by a hydrothermal reaction. Due to its special rod-like structure, which facilitated the transport of lithium ions and electrons, this material had an excellent electrochemical performance, and the reversible capacity remained at 628 mAh g^{-1} after 350 cycles [9]. Li Z's group prepared porous Co_3O_4 nanosheets using a template method and was still at 1380 mAh g^{-1} after 240 cycles [10]. Fan L's group synthesized porous Co_3O_4 nanofibers by electrospinning [11]. Wang D's group prepared a Co_3O_4 hollow sphere structure in the absence of a template and found that the hollow structure exhibited excellent lithium storage performance as an anode material for lithium-ion batteries [12]. Li L's group reacted cobalt chloride at 160°C for 24 hours without calcining the $\text{Co}(\text{OH})_2$ intermediate, and finally prepared nanodisks, nanobelts and other morphologies [13]. He M's group used a simple hydrothermal method to synthesize Co_3O_4 nanoarrays with a controllable morphology on nickel foam [14].

In this work, spherical Co_3O_4 (S- Co_3O_4) and amorphous coexisting sheet-spherical Co_3O_4 (S-S- Co_3O_4) were prepared without templates by a facile chemical deposition-calcination method. The method for preparing materials in an aqueous medium at room temperature has a simple preparation method and low cost. The experimental results show that, in comparison, S-S- Co_3O_4 has a higher reversible capacity with better cycling performance.

2. EXPERIMENT

2.1 Preparation of materials

The preparation of cobalt hydroxide with different morphologies is shown below. First, 0.2 g of polyvinyl pyrrolidone (PVP) was placed in a 250-ml three-necked flask containing a magnetic stirrer, and 100 mL of deionized water was measured. After the above solution was stirred uniformly, 0.0189 g of sodium borohydride was measured and dissolved in 38 mL of an aqueous solution containing 12 mL of aqueous ammonia (36%, AR) and in 35 mL of an aqueous solution containing 15 mL of aqueous ammonia (36%, AR). The former solution prepared spherical cobalt hydroxide, and the latter prepared flaky cobalt hydroxide. During the whole reaction process, argon gas was introduced to avoid oxidation. After reacting for 2 hours, it was found that the two solutions changed from pink to colorless, and a large number of blue-green precipitates and yellow-green precipitates were generated, indicating that the reaction was completed. The former phenomenon indicated that spherical cobalt hydroxide was produced, and the latter phenomenon indicated that flaky cobalt hydroxide was prepared. After centrifugally washing the product with deionized water five times, the product was dried to obtain cobalt hydroxide materials with different morphologies. The prepared cobalt hydroxide

material was finally calcined at 450°C for 2 hours to obtain tricobalt tetroxide materials with different morphologies.

2.2 Characterization of the Co_3O_4

The phase determination of the sample was identified using X-ray diffraction (XRD). The phase and crystal structure of each material were analyzed using a Miniflex X-ray diffraction analyzer produced by Rigaku Corporation of Japan. Field emission scanning electron microscopy FESEM was used to observe the microstructure and particle size of the material. A QUANTA F250 field emission scanning electron microscope from the American FEI company was used. vs. Li/Li^+

2.3 Electrochemical measurements

A CR2016 button cell was assembled in an argon atmosphere with a lithium sheet as a symmetrical electrode. The working electrode was made of Co_3O_4 , acetylene black (super P) and polyvinylidene fluoride (PVDF) with a weight ratio of 80:10:10 to make a uniform slurry. The solvent was an oily solvent, N-methyl pyrrolidone (NMP), and the separator is a polypropylene resin film. The electrolyte composition was 1 M LiPF_6 , which was dissolved in a solvent containing a 1:1 mixture of ethylene carbonate (EC) and diethyl carbonate (DEC). The battery in the test system (LAND CT 2001A) was subjected to a constant current charge-discharge cycling performance test with an electrochemical window of 0.01 and 3.0 V (vs. Li/Li^+).

3. RESULTS AND DISCUSSION

XRD patterns of S- $\text{Co}(\text{OH})_2$ and S-S- $\text{Co}(\text{OH})_2$ are shown in Figure 1 (a). The diffraction peaks of the materials at 19.0°, 23.9°, 32.4°, 37.8°, and 51.4° correspond to the (001), (100), (011), (012) and (111) crystal planes of standard cobalt hydroxide, respectively (JCPDS: 01-089 -8616). This indicates that the products obtained by this method are cobalt hydroxide. In comparison, S-S- $\text{Co}(\text{OH})_2$ has a relatively stable baseline with strong peak strength, which indicates that it has good crystallinity with relatively few spherical impurities. XRD patterns of S- Co_3O_4 and S-S- Co_3O_4 are shown in Figure 1 (b). Among them, 31.0°, 36.7°, 44.4°, 59.2°, and 65.3° can perfectly match the (220), (311), (400), (511), (440) crystal planes of the Co_3O_4 (JCPDS: 01-074- 1657), respectively. This shows that the products obtained by this method are both tricobalt tetroxide. Among them, S-S- Co_3O_4 has a (111) crystal plane at 19.1°, which may be caused by the presence of sheet materials [15]. After calcination, the baselines of the two materials were slightly flattened, indicating that the crystallinity of the materials increased during the calcination process. Compared with the spherical materials, the XRD baseline of S-S- Co_3O_4 is flatter. This finally indicates that the coexisting sheet and spherical materials with a coexisting sheet and spherical morphology have better crystallinity with fewer impurities.

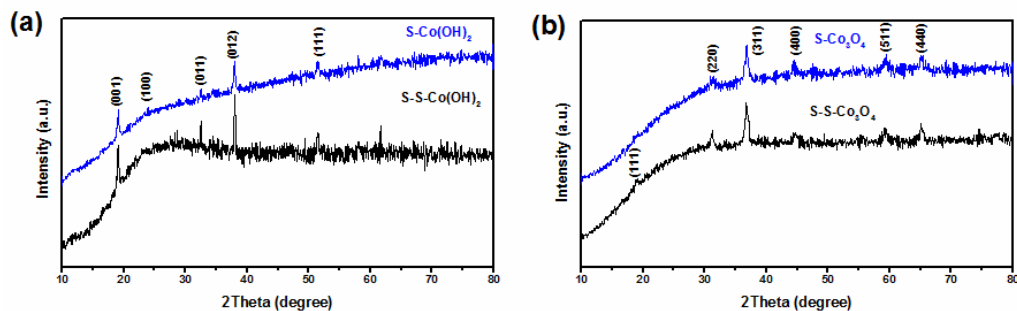


Figure 1. (a) XRD patterns of S-Co(OH)₂ and S-S-Co(OH)₂ and (b) XRD patterns of S-Co₃O₄ and S-S-Co₃O₄.

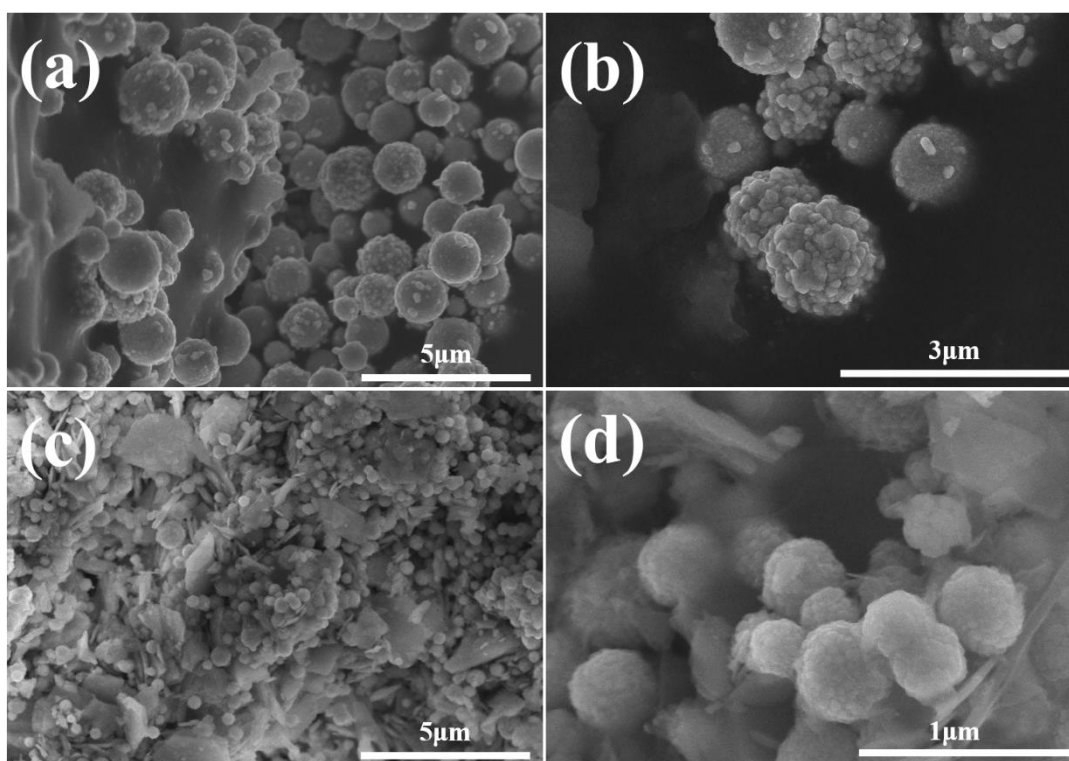


Figure 2. FESEM images of S-Co(OH)₂ (a and b) at different magnifications, while FESEM images of S-S-Co(OH)₂ (c and d) at different magnifications.

Figure 2 shows the morphological characterization of the prepared S-Co(OH)₂ and S-S-Co(OH)₂. It can be seen that S-Co(OH)₂ has a spherical shape with a more uniform particle size, and the secondary particle size is approximately 1-2 μm. The surface of most particles is rough, which is related to the agglomeration of many small particles. These primary particles are approximately 100-300 nm in size. The small spherical particles of S-S-Co(OH)₂ have smooth surfaces, but the surface is formed by a dense agglomeration of small particles. It can be seen from the figure that the material is composed of amorphous flakes and spherical particles. The amorphous flaky particles have a thin wall with a thickness of less than 100 nm. The spherical particles have a secondary particle diameter of approximately 200-500 nm, and the primary particle diameter is below 100 nm with a uniform particle size distribution. To confirm whether these spheres are aggregates formed by the agglomeration of

small particles, we performed a cross-sectional image analysis with FESEM. Figure 3 shows a cross-sectional FESEM image of a spherical particle. It can be seen from this figure that the prepared spherical particles are solid particles. These solid particles are not completely formed by the aggregation of small particles, but rather, a layer of small particles is agglomerated on the surface.

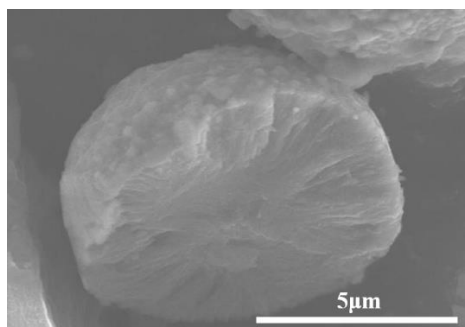


Figure 3. FESEM image of a S-Co(OH)₂ cross section.

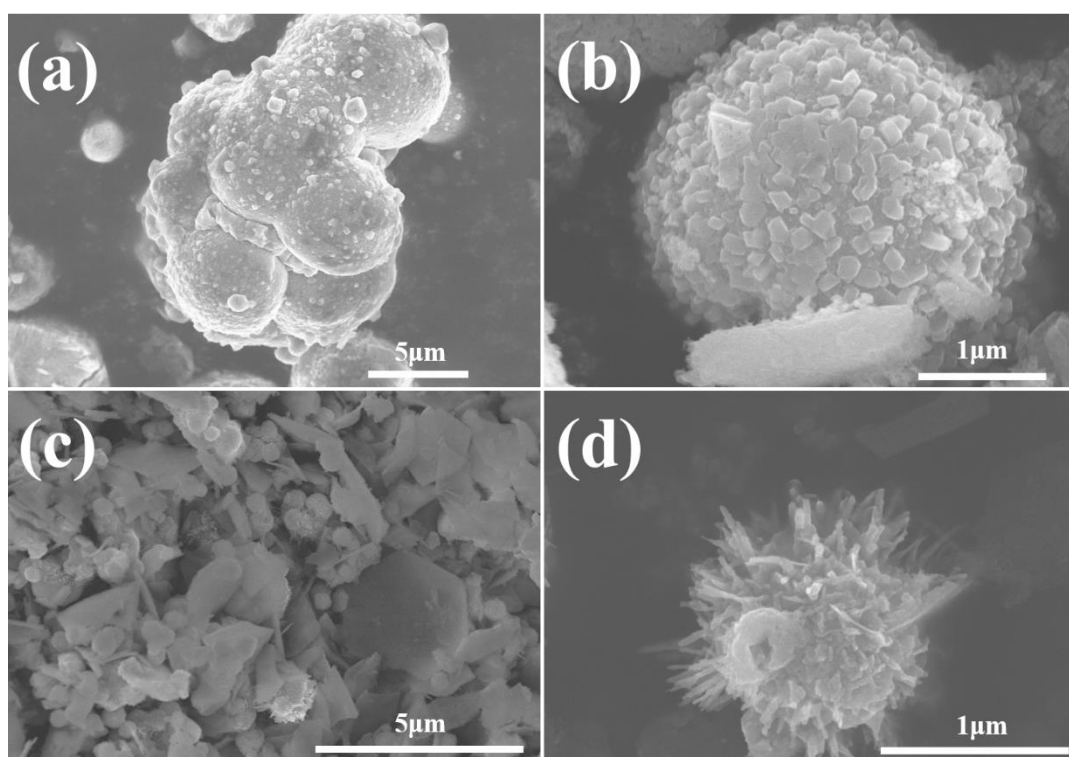


Figure 4. FESEM images of S- Co₃O₄ (a and b), while FESEM images of S-S- Co₃O₄ (c and d).

The FESEM image of cobalt tetroxide obtained after calcination of cobalt hydroxide at 550°C is shown in Figure 4. By comparison before calcination, it is found that the particle size after calcination has increased to approximately 3-5 µm. Some spherical particles agglomerate during the calcination process. The particles accumulated on the surface layer are recrystallized during calcination to form more angular particles on the particle surface. It can also be seen that the thickness of the sheet layer increases after calcination. After calcination, the secondary particle size of the spherical particles increased, and some particles with rough surfaces grow burr-like structures. The surface of the sheet

structure becomes porous, and these pores are helpful for alleviating the severe volume expansion caused by lithium-ion insertion. All of these unique properties improve the cycle life of the battery and lead to good electrochemical performance.

Figure 5 and Table 1 show the performance comparison of two different morphologies of Co_3O_4 . Among them, S-S- Co_3O_4 (Figure 5 (a)) has the best cycle performance. Its first charge-discharge capacity is 860 / 1089 mAh g^{-1} , first coulombic efficiency is 79%, and 50 cycles discharge capacity is 604 mAh g^{-1} with a capacity retention of 70%. In comparison to S-S- Co_3O_4 , S- Co_3O_4 has a poorer cycling performance. Its first charge-discharge capacity is 787 / 999 mAh g^{-1} , first coulombic efficiency is 79%, and discharge capacity after 50 cycles is 507 mAh g^{-1} with a capacity retention of 64%. In conclusion, it can be found that S-S- Co_3O_4 has better electrochemical performance than S- Co_3O_4 . This may be due to S-S- Co_3O_4 having a sheet-like morphology with a porous surface and a large specific surface area, which can alleviate the volume expansion caused by lithium-ion insertion and more easily promote electron and lithium-ion transmission. Therefore, S-S- Co_3O_4 shows a better electrochemical performance.

Table 2 lists the cycling performances of S- Co_3O_4 and S-S- Co_3O_4 studied in this work and the cycling performance of Co_3O_4 prepared by different methods as the anode of lithium-ion batteries. Before this work, Co_3O_4 has been widely used in lithium-ion batteries anodes. Among them, Binotto G's group synthesized Co_3O_4 by the precipitation method and found that super P mixed materials in organic solvents, which showed an excellent electrochemical performance (the first cycle provided 800 mAh g^{-1}) [16]. Huang G's group used the triethanolamine hydrothermal method to prepare micro-nano structured Co_3O_4 , which was a micro-cube structure composed of irregular nanoparticles with 1298 mAh g^{-1} at 0.1 C [17]. Fan X's group transformed $\text{Co}(\text{OH})_2$ nanosheets into porous Co_3O_4 nanosheets by calcination at high temperature. The research found that the morphology and electrochemical property could be significantly affected by different heat treatment temperatures [18]. Tong G's group synthesized Co_3O_4 through a bubble-assisted self-assembly technique and controlled morphological changes by increasing the decomposition temperature. The discharge capacity was 1467.9 mAh g^{-1} at a current density of 35 mA g^{-1} [19]. Yan D's group used the biological template method to infiltrate $\text{Co}(\text{NO}_3)_2$ into cotton fibers to synthesize tubular Co_3O_4 , and the prepared materials still maintained the morphology of raw cotton. Its specific capacity was 311.2 mAh g^{-1} after 80 cycles [20]. Wang H's group used metal phthalocyanine as a precursor and template to prepare transition metal oxide nanoparticles and the derived Co_3O_4 had an initial capacity of 1132.9 mAh g^{-1} at 50 mA g^{-1} [21]. Liang M's group synthesized layered Co_3O_4 by a hydrothermal method assisted by carbon spheres and hydroxypropyl cellulose, which showed an excellent cycling performance, and maintained a reversible capacity of 734.64 mAh g^{-1} after 500 cycles [22]. Ding H's group reported that a hollow $\text{Co}_3\text{O}_4@ \text{TiO}_2$ nanostructure could be synthesized using a metal-organic framework as a template. This structure significantly improved the cycle performance of the battery. After 100 cycles, it was 1057 mAh g^{-1} at 100 mA g^{-1} [23]. Zeng H's group used anthracite as a carbonaceous precursor and then synthesized nitrogen-doped porous Co_3O_4 /anthracite-derived graphene nanocomposites through an independent loading and heat treatment processes with a reversible capacity of 845 mAh g^{-1} [24]. Kong L's group synthesized Co_3O_4 with different aggregation forms by the co-precipitation method. Flower-like Co_3O_4 had a capacity of 910.7 mAh g^{-1} after 500 cycles [25].

The above synthesis method has many apparent disadvantages. The high cost of the template method is not suitable for large-scale industrialization, the low heating temperature of the hydrothermal method will lead to a poor crystallinity, the long time for calcination at high temperature will increase the energy consumption, and the carbon doping or coating preparation will decrease the specific capacity density. In this work, spherical Co_3O_4 (S- Co_3O_4) and amorphous coexisting sheet-spherical Co_3O_4 (S-S- Co_3O_4) were prepared without templates by a facile chemical deposition-calcination method. In this way, not only the morphology of the material is effectively controlled, but also the precursor can be prepared at room temperature, which makes the method relatively simple, low cost, and energy efficient. At the same time, the use of organic solvents is avoided, and the preparation process is more environmentally friendly. In addition, the prepared material also has an excellent electrochemical performance. Its discharge capacity of Co_3O_4 in the first cycle can reach 1089 mAh g^{-1} with the first coulombic efficiency is 79%, and 50 cycles discharge capacity is 604 mAh g^{-1} with a capacity retention of 70%.

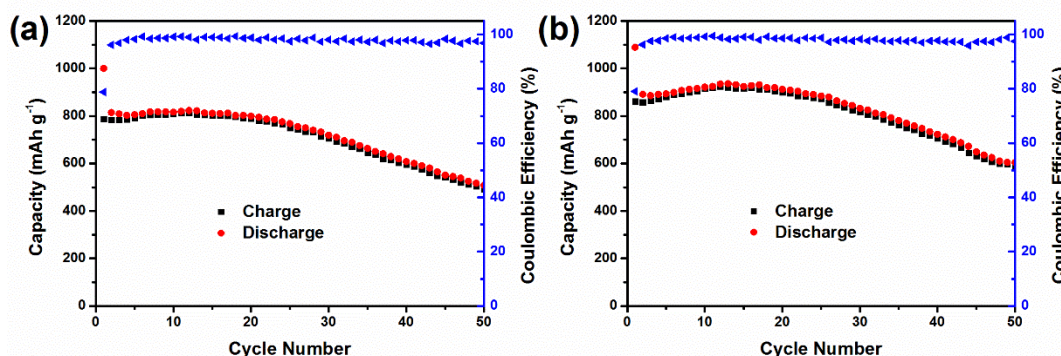


Figure 5. Cycling performance of (a) S- Co_3O_4 and (b) S-S- Co_3O_4 at a current density of 100 mA g^{-1} .

Table 1. Comparison of cycling performance between S- Co_3O_4 and S-S- Co_3O_4 .

	S-S- Co_3O_4	S- Co_3O_4
First discharge capacity (mAh g^{-1})	1089	999
First charge capacity (mAh g^{-1})	860	787
Coulomb efficiency for the first time (%)	79	79
50 cycling discharging capacity (mAh g^{-1})	604	507
50 cycling capacity retention rate (%)	70	64

Table 2. The results of this experiment are compared with the anodes of other Co₃O₄ lithium-ion batteries.

Sample	Cyclic stability	Reference
S-S-Co ₃ O ₄	604 mAh g ⁻¹ at 100 mA g ⁻¹ (50 cycles)	Present work
Porous Co ₃ O ₄ nanostructures	980 mAh g ⁻¹ at 50 mA g ⁻¹ (30 cycles)	[26]
Porous hierarchical spherical Co ₃ O ₄	300 mAh g ⁻¹ at 300 mA g ⁻¹ (20 cycles)	[27]
Co ₃ O ₄ polyhedral architectures	432 mAh g ⁻¹ at 50 mA g ⁻¹ (45 cycles)	[28]
Co ₃ O ₄ mesoporous microdisks	765 mAh g ⁻¹ at 100 mA g ⁻¹ (30 cycles)	[29]
Mesoporous Co ₃ O ₄ Nanoflakes	806 mAh g ⁻¹ at 0.1 C (300 cycles)	[30]
Co ₃ O ₄ /Co nanoparticles enclosed graphitic carbon	686 mAh g ⁻¹ at 100 mA g ⁻¹ (60 cycles)	[31]

4. CONCLUSIONS

In this work, spherical-Co(OH)₂ and amorphous coexisting sheet-spherical Co(OH)₂ were simply prepared at room temperature by using an aqueous solution. After calcination, S-Co₃O₄ and S-S-Co₃O₄, which correspondingly maintain their original shape, were successfully obtained. It avoids the high-temperature reaction and introduction of templates, which are common in traditional synthesis procedures; thus, the reaction process is easier and saves energy. At the same time, the use of organic solvents is avoided, and the preparation process is more environmentally friendly, less toxic and harmless. By comparing the electrochemical performances of the two cobalt tetroxides with different morphologies, it is found that S-S-Co₃O₄ exhibits excellent electrochemical performance. The first discharge capacity is 1089 mAh g⁻¹ with a first coulombic efficiency of 79%. S-S-Co₃O₄ has good and a porous surface. This will increase the specific surface area, reduce the volume expansion caused by lithium-ion insertion and extraction, and more easily promote electron and lithium-ion transmission. The above properties make the electrochemical reaction proceed more easily, so it has a high capacity and good cycle life. These advantages make S-S-Co₃O₄ a promising anode material for lithium-ion batteries; moreover, the preparation method is simple and efficient and can be generalized to other electrode materials with different morphologies.

ACKNOWLEDGMENTS

This work was financially supported by the National Natural Science Foundation of China (No. 21965017 and 51764029), the Provincial Natural Science Foundation of Yunnan (No. 2017FB085 and 2018FB087).

References

1. T. Ohzuku and A. Ueda, *Solid State Ionics*, 69 (1994)201.
2. H, Li, X. J. Huang and L. Q. Chen, *Electrochem. Solid-State Lett.*, 1(1998)241.

3. M. Nagayama , T. Morita , H. Ikuta , M. Wakihara , M. Takano and S. Kawasaki, *Solid State Ionics*, 106(1998)33.
4. Ian A. Courtney, R.A. Dunlap and J.R. Dahn, *Electrochim. Acta*, 45(1999)51.
5. S. Y. Huang, L. Kavan, I. Exnar and M. Gratzel, *J. Electrochem. Soc.*, 142(1995)L142.
6. Y. Idota, M. Nishima, Y. Miyaki, T. Kubota and T. Miyasaka, *European: EP0651450* (1995).
7. J. J. Deng, X. X. Lv, J. Zhong and X. H. Sun, *Appl. Surf. Sci.*, 475(2019)446.
8. B. Wang, X. Y. Lu, C. W. Tsang, Y. H. Wang, W. K. Au, H. F. Guo and Y. Y. Tang, *Chem. Eng. J.*, 338(2018)278.
9. X. Li, X. D. Tian, T. Y. Song, Y. M. Liu, Q. G. Guo and Z. J. Liu, *J. Alloys Compd.*, 735(2018)2446.
10. Z. P. Li, X. Y. Yu and U. Paik, *J. Power Sources*, 310(2016)41.
11. L. Fan, W. D. Zhang, S. P. Zhu and Y. Y. Lu, *Ind. Eng. Chem. Res.*, 56(2017)2046.
12. D. L. Wang, Y. C. Yu, H. He, J. Wang, W. D. Zhou and H. D. Abruna, *ACS nano*, 9(2015)1775.
13. L. L. Li, Y. Chu, Y. Liu, J. L. Song, D. Wang and X. W. Du, *Mater. Lett.*, 62(2008)1507.
14. M. He, P. Zhang, S. Xu and X. B. Yan, *ACS Appl. Mater. Interfaces*, 8(2016)23713.
15. X. Li, G. L. Xu, F. Fu, Z. Lin, Q. Wang, L. Huang, J. T. Li and S. G. Sun, *Electrochim. Acta*, 96(2013)134.
16. G. Binotto, D. Larcher, A. S. Prakash, R. H. Urbina, M. S. Hegde and J. Tarascon, *Chem. Mater.*, 19(2007)3032.
17. G. Y. Huang, S. M. Xu, S. S. Lu, L. Y. Li and H. Y. Sun, *ACS Appl. Mater. Interfaces*, 6(2014)7236.
18. C. C. Liang, D. F. Cheng, S. J. Ding, P. F. Zhao, M. S. Zhao, X. P. Song and F. Wang, *Electrochim. Acta*, 142(2014)268.
19. G. X. Tong, Y. Liu and J. G. Guan, *J. Alloys Compd.*, 601(2014)167.
20. D. L. Yan, Y. Zhang, X. Y. Zhang, Z. Z. Yu, Y. Y. Zhao, G. S. Zhu, G. C. Chen, C. G. Ma, H. R. Xu and A. B. Yu, *Ceram. Int.*, 43(2017)9235.
21. H. G. Wang, Y. J. Zhu, C. P. Yuan, Y. H. Li and Q. Duan, *Appl. Surf. Sci.*, 414(2017)398.
22. M. M. Liang, M. S. Zhao, H. Y. Wang, F. Wang and X. P. Song, *J. Storage Mater.*, 17(2018)317.
23. H. Ding, X. K. Zhang, J. Q. Fan, X. Q. Zhan, L. Xie, D. Shi, T. Jiang and F. C. Tsai, *ACS Omega*, 4(2019)13241.
24. H. H. Zeng, B. L. Xing, L. J. Chen, G. Y. Yi, G. X. Huang, R. F. Yuan, C. X. Zhang, Y. J. Cao and Z. F. Chen, *Nanomater.*, 9(2019)1253.
25. L. L. Kong, L. Wang, D. Y. Sun, S. Meng, D. D. Xu, Z. X. He, X. Y. Dong, Y. F. Li and Y. C. Jin, *Mol.*, 24(2019)3149.
26. H. Sun, M. Ahmad and J. Zhu, *Electrochim. Acta*, 89(2013)199.
27. J. Zheng, J. Liu, D. Lv, D. P. Lv, Q. Kuang, Z. Y. Jiang, Z. X. Xie, R. B. Huang and L. S. Zheng, *J. Solid State Chem.*, 183(2010)600.
28. W. W. Yuan, D. Xie, Z. M. Dong, Q. M. Su, J. Zhang, G. H. Du and B. S. Xu, *Mater. Lett.*, 97(2013)129.
29. Y. H. Jin, L. Wang, Y. M. Shang, J. Gao, J. J. Li and X. M. He, *Electrochim. Acta*, 151(2015)109.
30. S. Q. Chen, Y. F. Zhao, B. Sun, Z. M. Ao, X. Q. Xie, Y. Y. Wei and G. X. Wang, *ACS Appl. Mater. Interfaces*, 7(2015)3306.
31. Z. L. Yan, Q. Y. Hu, G. C. Yan, H. K. Li, K. Shi, Z. W. Yang, X. H. Li, Z. X. Wang and J. X. Wang, *Chem. Eng. J.*, 321(2017)495.